JOURNAL OF AIRCRAFT
Vol. 33, No. 4, July–August 1996

Engineering Notes

ENGINEERING NOTES are short manuscripts describing new developments or important results of a preliminary nature. These Notes cannot exceed 6 manuscript pages and 3 figures; a page of text may be substituted for a figure and vice versa. After informal review by the editors, they may be published within a few months of the date of receipt. Style requirements are the same as for regular contributions (see inside back cover).

Seed Particle Dynamics in Tip Vortex Flows

J. Gordon Leishman*
University of Maryland,
College Park, Maryland 20742-3015

Introduction

LASER Doppler velocimetry (LDV) can alleviate many limitations imposed by conventional flow diagnostic probes, although the technique is by no means free from error. Yet, other than optical access, there is practically no limit to where measurements can be made. For example, it is possible to take measurements near to or in the plane of rotation of turbines, helicopter rotors, or propeller blades, something that would be impossible with other probes. However, LDV depends on signals produced by particles entrained into the flow that convect through a minute measurement volume as defined by pairs of interfering focused laser beams. It is generally assumed that these particles faithfully follow the flow, yet this is not always guaranteed.

General considerations in the selection of seed particles for LDV are discussed by Menon and Lai,[1] Dring,[2] and others. Depending on the particle mass and size, and the velocity field where it is entrained, a particle may acquire a velocity that is different to that of the fluid. The larger the particle the better the LDV signal-to-noise ratio, however, depending on the nature of the velocity field, the larger particles may be less likely to follow the flow. This is because of both viscous drag and inertial effects. The problem of particle size is especially acute with tip vortices generated by rotors, which tend to have small viscous cores and high rotational velocities near the vortex axis, and therefore, will subject the seed particles to finite centripetal and Coriolis accelerations. Entrained seed particles in this region will tend to spiral radially away from the vortex axis, and the LDV measurements will obviously be subjected to some velocity error. Even if one may be able to correct for this error through particle sizing techniques, the centrifugal forces on the particles results in a region of the flow deficient of seed,[3] and this leads to low data measurement rates.

Discussion

A representative set of LDV measurements made inside the tip vortex generated by a hovering rotor are shown in Fig. 1. Helicopter rotors tend to generate strong tip vortices, and quite vividly illustrate LDV seeding issues. In this case, three-component velocity measurements were made in a phase-resolved sense at various grids and distances behind the rotor blade.[4] The data in Fig. 1 show the instantaneous tangential (swirl) component of induced velocity (normalized by rotor tip speed) at two ages after the vortex was formed. The ordinate is the distance from the vortex axis normalized by the blade chord. Note the asymmetry of the velocity profiles, which is in part, because of the finite radius of curvature and the helical nature of the trailed vortex filament.

The corresponding measured relative particle count (ratio of local particle count in each grid bin to total particle count) of seed that pass through the LDV measurement volume is shown in the lower part of Fig. 1. The seed particles used were atomized olive oil with a statistical mean diameter of 0.6 μm. Note the interesting weighting of the particle statistics, with a bucket-shaped curve in each case indicating a significant seed void inside the vortex core. In general, the measured curves showed a maximum particle encounter frequency outside the vortex core, followed by an asymptotic decrease to a fairly constant value in the outer regions of the vortex.

The seed particle behavior inside a tip vortex can be examined numerically to give an estimate as to the significance of both particle velocity errors and the relative frequency of a seed particle passing through the measurement grid. Numerical solutions can also help in particle sizing selection for a given flow, and for estimating the time required to acquire a statistical minimum number of samples at each grid point. Assuming Stokes drag law ($Re_p < 1$, where Re_p is the particle Reyn-

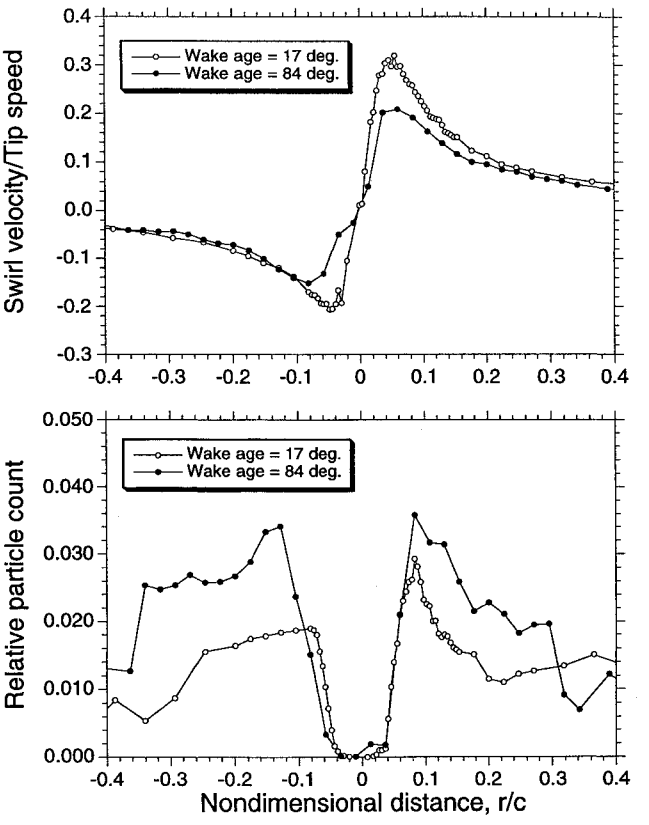

Fig. 1 Typical variations in swirl velocity profile and relative particle count measured through a rotor tip vortex at two wake ages after release.

Received Nov. 12, 1995; revision received Jan. 5, 1996; accepted for publication Jan. 15, 1996.

*Associate Professor, Glenn L. Martin Institute of Technology, Department of Aerospace Engineering. Senior Member AIAA.

olds number based on diameter) and spherical particles, then the differential equations of motion of a seed particle in a two-dimensional cylindrical flow with a prescribed swirl velocity V_θ and radial velocity V_r are given by Fuchs[5] as

$$\frac{dV_{r_p}}{dt} = \frac{V_{\theta_p}^2}{r} + \frac{1}{\tau_v}(V_r - V_{r_p}) \tag{1}$$

$$\frac{dV_{\theta_p}}{dt} = -\frac{2V_{\theta_p}V_{r_p}}{r} + \frac{1}{\tau_v}(V_\theta - V_{\theta_p}) \tag{2}$$

where V_{θ_p} and V_{r_p} are the corresponding swirl and radial components of the particle in the velocity field, respectively. The time constant τ_v is given by Refs. 5 and 6 as $\tau_v = \rho_p d_p^2/18\mu$, where ρ_p and d_p are the density and diameter of the seed particle, respectively. Note that these equations are coupled through the Coriolis term.

The previous differential equations can be integrated in time for a known (assumed) vortex flow, given some initial displacement and velocity conditions for the particle. For a simple forced vortex the equations can be integrated exactly and lead to spiral particle trajectories. Results for this special case are given by Kriebel.[3] For more general velocity fields, the integration must be performed numerically.

A key parameter affecting the centripetal accelerations in the flow and, therefore, the trajectory of seed particles, is the vortex strength. For a rotor, the tip vortex strength (circulation) Γ, can be related approximately to the blade loading (C_T/σ) by the expression $\Gamma = kc\Omega R(C_T/\sigma)$, where k is a constant, c is the blade chord, and R is the rotor radius. C_T is the rotor thrust coefficient, and σ the rotor solidity. Since most LDV measurements are made on model-scale rotors, the preceding expression can be used to deduce some interesting results, such as the likelihood of successfully seeding a given tip vortex flow. For example, for the same blade loading a one-fifth-geometrically scaled but full-Mach scaled rotor configuration will have a tip vortex strength (circulation) one-fifth that of the full-scale rotor. However, since both the model and full-scale rotor cases the viscous core radii are typically of the order of one-tenth the blade chord, this means that the centripetal accelerations inside the core of the model-scale rotor vortex will be larger, thereby making seeding issues more critical.

This is shown in Fig. 2, which shows the computed swirl and radial particle velocity ratios ($V_{\theta_p}/\omega r$ and $V_{r_p}/\omega r$, respectively) at both model and full-scale as a function of particle size inside a forced (fully rotational) vortex. In this case, for particles that follow the flow, $V_{\theta_p} = \omega r$ and $V_{r_p} = 0$. The calculations were performed using geometric and operational parameters typical of the UH-60 Blackhawk rotor, which generates a tip vortex strength of approximately 28 m^2s^{-1}. Note from Fig. 2 that the velocity errors at the model-scale are obviously much larger because of the higher centripetal accelerations. The most significant error is in the radial component of velocity, but for particles sizes of less than about 1 μm, the errors appear to be generally small.

Kriebel[3] has used the nondimensional parameter $A = \rho_p d_p^2 \omega/18\mu$ to address the significance of centrifugal effects on suspended seed particles. For a forced vortex, this parameter indicates the relative importance of inertial (centrifugal) to viscous drag forces. However, for a general vortex of strength Γ with a viscous core radius r_c, an alternative nondimensional parameter can be written as

$$\hat{A} = \rho_p d_p^2 \Gamma/\mu r_c^2 \tag{3}$$

and this quantity can be used to help define more precise relative sizing criteria for seed particles in vortical type flows. It is also noted from Eq. (3) that the seed-sizing issue becomes particularly critical for vortices with small core dimensions (small values of r_c), which is typical of those generated by propellers or helicopter rotors.

Typical results for the velocity error have been computed for different particle sizes released inside a tip vortex with a desingularized swirl velocity field approximated by

$$V_\theta(r) = \frac{\Gamma r}{2\pi\sqrt{r_c^4 + r^4}}, \qquad V_r = 0 \tag{4}$$

where r is the radial distance from the vortex axis. A value $\Gamma = 5.6$ m^2s^{-1} was assumed (UH-60 model-scale). The results in Fig. 3 are plotted as a function of radius measured from the vortex axis nondimensionalized by core radius. Again, it is clear that the radial velocity component is more significantly in error, but only for particle sizes of more than 1 μm. Inside the rotational core these errors remain nominally constant, but quickly diminish as the particle convects through the region of highest velocity and into the outer (irrotational) region of the vortex. The net effect of a number of particles being released into the vortex, say at various radial locations across the vortex axis, is that they tend to migrate radially outward across the (circular) streamlines from their original positions. For particles released inside the vortex core, the centrifugal forces cause the particles to spiral quickly outward creating a void. This is a well-known effect often noted in laser light sheet flow visualization experiments.[7] Farther away from the vortex axis, the particles follow more circular paths.

The corresponding particle count (frequency) distribution has been computed for different seed particle diameters using the differential equations of particle motion and with the previously defined vortex parameters. This helps give a quantifi-

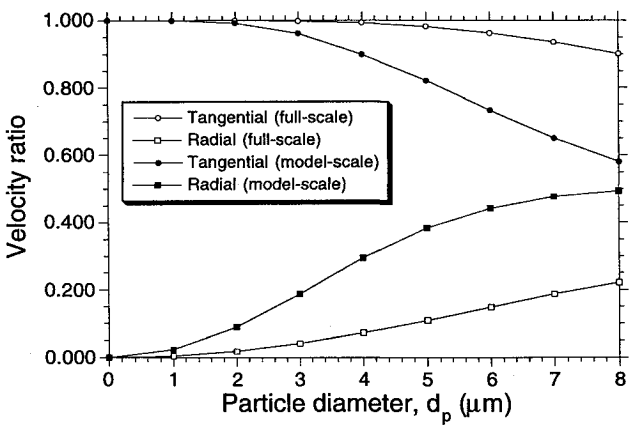

Fig. 2 Swirl and radial velocity errors vs particle size for a forced vortex.

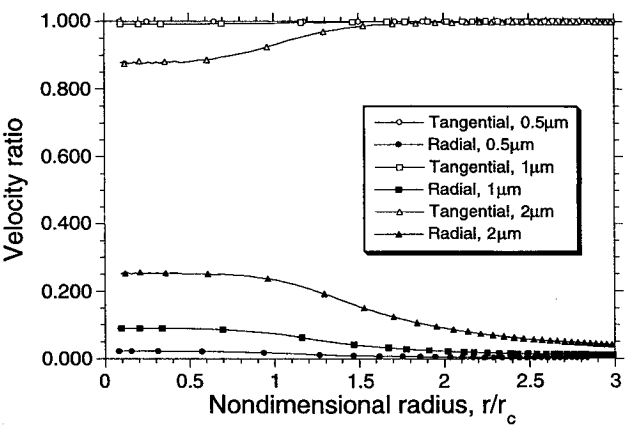

Fig. 3 Swirl and radial velocity errors vs radial location for various particle sizes inside a desingularized vortex, $\Gamma = 5.6$ m^2s^{-1}.

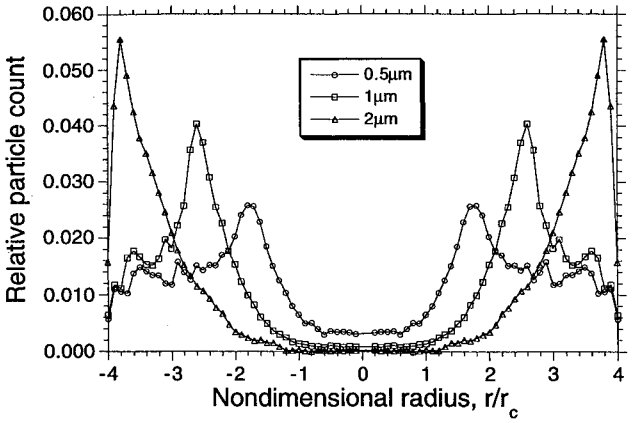

Fig. 4 Computed relative frequency of particles for various particle sizes inside a desingularized vortex, $\Gamma = 5.6\ m^2s^{-1}$.

able picture of the likelihood of being able to successfully seed a vortical flowfield, and also provides an indicator of the data rates and particle weighting count over the measurement grid that one would expect in practice. Data rates are particularly important for rotor tests because of the typically long time scales involved. These particle trajectory calculations were conducted by releasing a large number of uniformly dispersed particles inside the prescribed vortex flowfield at time zero, and integrating the equations of motion in time until the particles spiraled out of the computational grid.

The computed results are shown in Fig. 4 in the form of relative particle count as a function of nondimensional distance from the vortex axis. Note the similarities of these computed results to the measurements shown in Fig. 1. As discussed previously, inside the vortex core ($r/r_c < 1$), the centripetal accelerations cause the particles to spiral quickly outward, creating a seed void. Inside this void, data rates are obviously relatively low, which in practice leads to very long elapsed time frames to acquire measurements to the necessary statistical precision. Note that the particles that are initially released inside the rotational core reach an equilibrium somewhere outside the core, with a much higher overall relative frequency being obtained in these regions. The radial position and magnitude of this peak are strongly dependent on particle size, with the larger particles being centrifuged considerably further outward from the vortex axis.

Conclusions

Experiments and calculations have been conducted to explore issues associated with seeding of strong vortical flows for LDV measurements, such as flows induced by the tip vortices generated by rotors. Both velocity errors and statistical weighting of the seed distribution through the vortex have been examined. Radial velocity errors tend to be larger than swirl errors, and dominate up to two core radii from the vortex axis. The weighting of seed is such that the core (rotational) region suffers a scarcity of particles, with a peak in the density distribution well outside the viscous core. This distribution is very sensitive to particle mass and size. A nondimensional parameter $\hat{A}$ has been developed to help quantify the likelihood of successfully seeding a typical vortex flow.

References

[1]Menon, R., and Lai, W. T., "Key Considerations in the Selection of Seed Particles for LDV Measurements," *Laser Anemometry Advances and Applications*, Vol. 2, *4th International Conference on Laser Anemometry* (Cleveland, OH), 1991, pp. 719–730.

[2]Dring, R. P., "Sizing Criteria for Laser Anemometry Particles," *Journal of Fluids Engineering*, Vol. 104, March 1982, pp. 15–17.

[3]Kriebel, A. R., "Particle Trajectories in a Gas Centrifuge," *Journal of Basic Engineering*, Vol. 83, No. 3, 1961, pp. 333–340.

[4]Leishman, J. G., Baker, A., and Coyne, A., "Measurements of Rotor Tip Vortices Using Three-Component Laser Doppler Velocimetry," *Proceedings of the 2nd International Aeromechanics' Specialists' Conference, American Helicopter Society* (Bridgeport, CT), 1995, pp. 37–57.

[5]Fuchs, N. A., *The Mechanics of Aerosols*, Pergamon, Oxford, England, UK, 1964.

[6]Buchhave, P., George, K. W., and Lumley, J. L., "The Measurement of Turbulence with the Laser Doppler Anemometer," *Annual Review of Fluid Mechanics*, Vol. 11, 1979, pp. 443–503.

[7]Ghee, T. A., and Elliott, J. W., "A Study of the Rotor Wake of a Small-Scale Rotor Model in Forward Flight Using Laser Light Sheet Flow Visualization with Comparisons to Analytical Models," *Proceedings of the 48th Annual Forum of the American Helicopter Society*, Washington, DC, 1992.

Effects of Leading-Edge Sweep Angle on Nonzero Trimmed Roll Angles

Eric J. Stephen* and Drew A. Sopirak†
U.S. Air Force Academy, Colorado 80840

Introduction

RECENTLY, there has been interest in improving aircraft maneuverability through the exploitation of unsteady aerodynamics and thrust vectoring. These techniques can extend the flight envelope to near or even into the poststall flight regime. The extension of the flight envelope increases the need for understanding high-angle-of-attack aerodynamics.

The focus of this study was the roll stability of delta wings at high angle of attack. The symmetry of the delta wing suggests roll stability at 0 deg of roll only, but Hanff and Jenkins[1] showed that at a high incidence angle ($\sigma = 30$ deg) a 65-deg delta wing was statically stable at ± 21 deg of roll as well as at 0 deg. Further experiments from Hanff, reported by Jenkins,[2] showed that one-, two-, or three-trimmed roll positions could be produced by changing the model incidence angle. Similar explanations of this phenomenon were provided by Stephen[3] and Ericsson.[4] The current set of experiments was designed to test Stephen's[3] conceptual model and show the effects of sweep angle changes on roll stability.

Free-to-roll experiments were limited to moderately swept delta wing models to avoid wing rock. Three flat-plate delta wing models were tested ($\Lambda = 55$, 60, and 65 deg). The 65-deg model allowed for comparison with previous work.[1,2,4,5] A flat plate 65-deg delta wing with a splitter plate and a scale model F-117 with 67-deg sweep were also tested to determine the effect of more complicated geometries on the trimmed roll positions. Besides the trimmed roll data, examination of the roll trajectories suggested some characteristics of the dynamic flow response.

Methods

Each of the three flat plate models had a root chord length of 10 in. and a thickness of 0.125 in. The leading and trailing edges were beveled from the top and bottom with a 22.5-deg

Presented as Paper 94-1885 at the AIAA 12th Applied Aerodynamics Conference, Colorado Springs, CO, June 20–23, 1994; received July 25, 1995; revision received Feb. 16, 1996; accepted for publication Feb. 16, 1996.

*Frank J. Seiler Research Laboratory, Unsteady Aerodynamics Task Manager; currently Chief, Performance Assessment and Analysis Branch, SBIR Systems Program Office, 185 Discoverer Blvd., Suite 2512, Los Angeles AFB, CA 90245-4695. Member AIAA.

†Cadet, Frank J. Seiler Research Laboratory. Student Member AIAA.